Networked Acoustic Modems for Real-Time Data Delivery from Distributed Subsurface Instruments in the Coastal Ocean: Initial System Development and Performance

DANIEL L. CODIGA

Department of Marine Science, University of Connecticut, Groton, Connecticut

JOSEPH A. RICE

Department of Physics, Naval Postgraduate School, Monterey, California

PAUL A. BAXLEY

Acoustics Branch, Space and Naval Warfare Systems Center, San Diego, California

(Manuscript received 8 January 2002, in final form 15 March 2003)

ABSTRACT

Results are reported from field tests of networked acoustic modems used for wireless real-time delivery of oceanographic measurements from a distributed array of subsurface instruments in coastal waters. The network demonstrated consists of sensor nodes, repeater nodes, gateway nodes, and a shore-based control center. Sensors are oceanographic instruments interfaced with acoustic modems, deployed in trawl-resistant bottom frames with azimuthally omnidirectional acoustic signaling needed for flexible network rerouting. Repeaters are individual acoustic modems to relay data so the array covers a larger area; only these relatively low-cost nodes are suited for deployment unprotected from trawlers. Gateways are buoys with acoustic modems interfaced to cellular telephone modems for communication between the underwater network and the shore. The experiment site is the inner continental shelf off Montauk Point, New York, and Block Island, Rhode Island, with a U.S. Coast Guard navigation buoy equipped as a gateway. Conditions span a variety of sound-speed profiles, water depths (~25–50 m), and seasons. Long-term average rates of successful transmissions fall to about 50% at a range of 3–4 km in the typically adverse shallow-water acoustic channel. This is adequate for networked acoustic modems to be cost effective in providing quantities of data typically required for data assimilative modeling of coastal oceanographic processes. Modem range degrades in association with increased winds; numerically modeled rays indicate that direct paths between nodes commonly do not exist. Networking functions demonstrated include handshaking protocols, receive-all gateway mode, and rerouting of data pathways from shore in response to a repeater node that is trawled out.

1. Introduction

Technologies to collect data from the coastal ocean in real time are important to a broad societal cross section including academic researchers, the military, resource managers, and marine safety and commercial operators. Along with advances in basic scientific understanding, examples of applications for real-time measurements include improved management of accidents involving hazardous materials and more effective environmental monitoring. For ocean surface properties, measurement techniques have matured. For example, satellites routinely sense surface temperatures and optical properties, and high-frequency radar can remotely measure coastal surface currents from shore towers. Such data are well suited for real-time distribution since they are collected via platforms having reliable and frequent communication with shore, or residing on land.

In contrast to surface measurements, real-time collection of subsurface data from multiple distributed instruments presents a major remaining challenge. To address this is crucial because water-column measurements resolving vertical structure are essential to understanding many coastal oceanographic processes. For example, a thin surface layer of buoyant flow with dynamics uncoupled from deeper flow often occurs across coastal areas influenced by estuarine outflows. Surface measurements will shed little light on the majority of the water column beneath this shallow layer.

There is a clear need for a system to deliver data from multiple subsurface instruments distributed across areas of the coastal ocean in real time. In many contexts, a primary goal is to provide input for regional data as-

Corresponding author address: Dr. Daniel L. Codiga, University of Connecticut, Avery Point Campus, 193 Marine Science Bldg., 1084 Shennecossett Rd., Groton, CT 06340.
E-mail: d.codiga@uconn.edu

similative numerical modeling of circulation and ecosystem processes. Field sampling required for effective assimilative modeling depends on the focus of any given study, but typical needs are for (a) instrument locations that span a region 10–20 km across, in order to capture spatial variations in circulation and water properties, and (b) measurements that are delivered at least several times daily, in order to resolve tidal fluctuations and enable separation of nontidal variability from the nearly deterministic tidal changes that can be dominant.

A number of operational impediments must be confronted: severe winds, strong tidal currents, mobile sediments, heavy commercial shipping and fishing activities, rapid biofouling processes, as well as recreational traffic that increases the likelihood of equipment tampering and pilfering. Seafloor wires and cables are incompatible with bottom-fishing activities. Acoustic modems present a wireless alternative; Stojanovic (1996) and Kilfoyle and Baggeroer (2000) provide reviews of underwater acoustic telemetry advances. For example, one-way data transfers can be made from instruments directly to surface buoys at or near each instrument for relay to shore (Frye et al. 1999).

A networked acoustic modem system (e.g., Curtin et al. 1993; Catapovic et al. 1993) is a focus of the Front-Resolving Observation Network with Telemetry (FRONT) project (information online at http://www.nopp.uconn.edu), a collaboration of the University of Connecticut; the Space and Naval Warfare Systems Center in San Diego, California; and Benthos, Inc. The system relies on acoustic telemetry and ranging advances pursued by the U.S. Navy for undersea surveillance that is referred to in general as ''telesonar'' technology (e.g., Green et al. 1998b). The FRONT site spans depths of about 20–60 m on the inner continental shelf outside Block Island Sound, a region with complex bathymetry, strong tidal currents, and buoyant estuarine outflows. A sharp gradient or front in oceanic properties roughly along the 50-m isobath is commonly seen in satellite sea surface temperatures (Ullman and Cornillon 1999) and motivated the initially proposed array design (Fig. 1a).

The network involves telesonar modems deployed in conjunction with three types of nodes, as depicted schematically in Fig. 1b for the initially proposed FRONT array. Sensor nodes are oceanographic instruments connected serially to an acoustic modem to transmit data through the network at regular intervals. Gateways are surface buoys serving as the link between the subsurface network and the shore. Repeater nodes are individual acoustic modems serving only to relay data packets. Sensor and gateway node modems are also capable of relaying data.

Networked acoustic modems offer a number of advantages for this application. Use of repeater nodes allows larger sensor separation and hence greater spatial coverage. Repeaters also enable multiple data routes to shore from each sensor. Two-way real-time communication between the shore and the subsurface network facilitates reconfiguration of data routing, enabling the network to accommodate unanticipated loss or failure of an individual repeater—for example, due to tampering, or by impact of trawling gear—by changing to secondary routes. Multiple gateway nodes mean the reconfiguration capability applies to failure of a gateway. Two-way communication also makes adaptive sampling possible. The network is expandable and with additional repeaters allows sensors to be placed at increasing distances from the gateway; each gateway serves multiple instruments so the number of system components subject to the problematic sea surface environment is minimized. Gateways can be configured to ''overhear'' all network communication, so a data packet transmitted at each of multiple hops along a route to the gateway has redundant opportunities to reach the gateway. Finally, certain sensors can be deployed in bottom frames designed to protect against fishing gear impacts.

For FRONT, packets are nominally a few hundred bytes in size and sent from each sensor node nominally each hour or two. Transmissions are therefore sufficiently infrequent that the time-delay multiple access (TDMA) network design is impacted by the disadvantage of transmission latency (Kilfoyle and Baggeroer 2000) quite weakly. Mean time to failure (MTTF) for the network due to power consumption is a function of data packet size and how often they are sent. Reliance of gateways on solar panels allows unattended operation for extended duration; for example, at least 6 months of operation has been demonstrated in FRONT. Sensors and repeaters, powered by onboard batteries, have operated for 3–6-month periods; larger battery packs could straightforwardly extend this to at least a year. While FRONT incorporates network maintenance cruises each 3 months, a 1-yr network MTTF is feasible.

The primary constraint on the network is that the adverse acoustic channel (e.g., Catipovic 1990) limits communication over horizontal distances, and effects such as multipathing and fading (e.g., Proakis 1991) that must be overcome can be severe in shallow coastal areas (e.g., Rice 1997). A network of acoustic modems is not likely to be cost effective in achieving spatial coverage across areas spanning 10–20 km unless its nodes can be separated by at least several kilometers, because otherwise the large number of nodes becomes impractical. Yet, over distances of a few kilometers or more, refraction makes it possible that no direct acoustic path between nodes will exist so that acoustic rays are forced to interact with the surface and/or bottom boundaries at least once. In addition, coastal areas have highly variable sound-speed profiles owing to wind-driven, estuarine, and tidal mixing processes, as well as high and variable

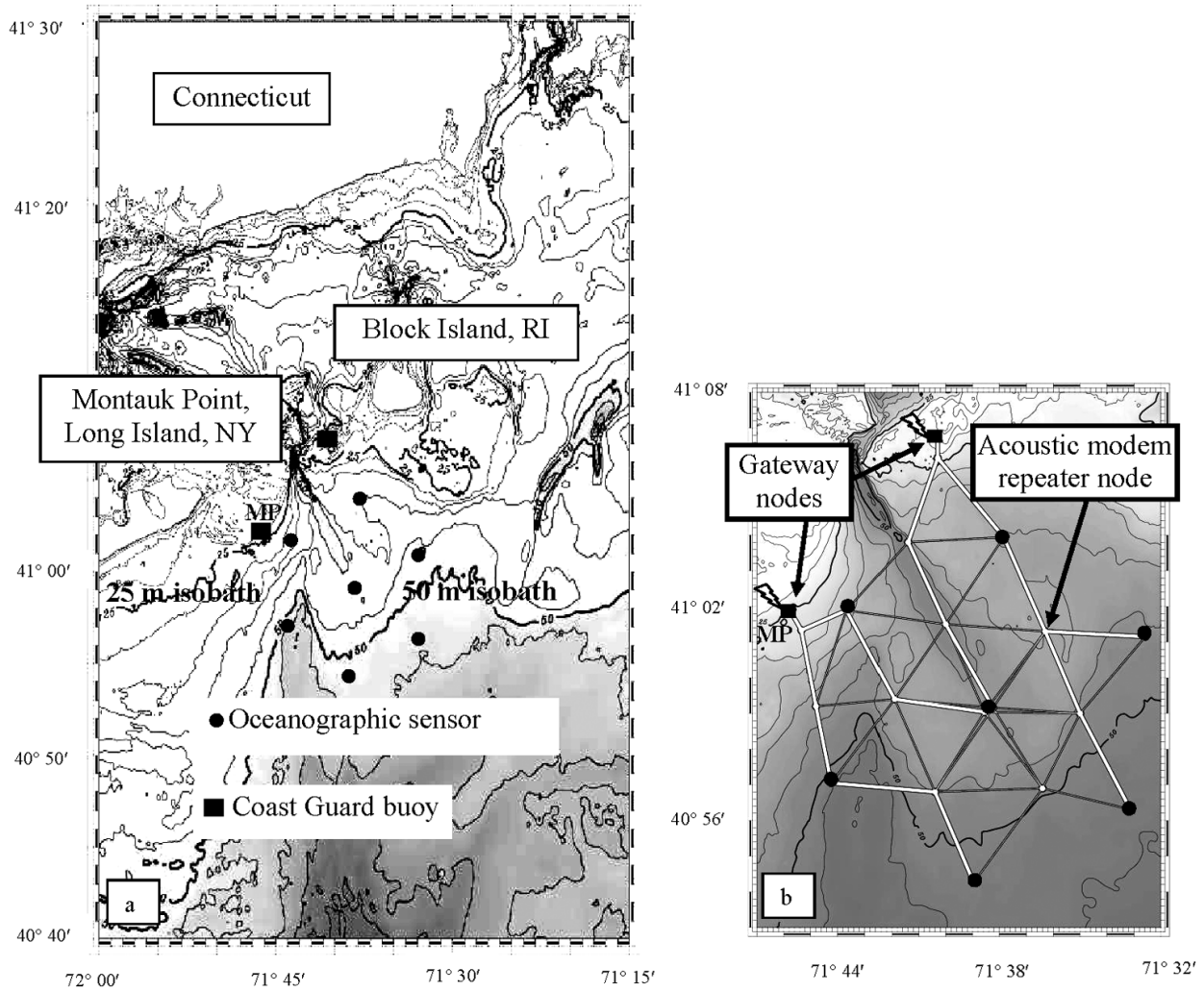

FIG. 1. (a) Site of the FRONT study on the inner continental shelf outside Block Island Sound. In its initially proposed configuration shown here, the array of subsurface oceanographic instruments spans a region 18–20 km across and includes sensor separations of about 9 km. (b) Schematic of networked acoustic modems for real-time wireless data delivery from the array in (a). Gateway nodes are buoys that provide two-way communication between the shore and the subsurface network via cellular modem. Acoustic modems deployed with each sensor send data to the gateways along primary routes (white lines). Routes span multiple acoustic links and form a binary tree network topology. Acoustic modems deployed singly act as repeater nodes, or relays, between sensor nodes to reduce transmission distances (to about 5 km in this depiction). Failure or loss of an individual repeater or gateway is accommodated by reconfiguring routes along secondary pathways (thin lines).

levels of ambient noise associated with commercial shipping activity.

This article first presents trawl-resistant bottom frame and gateway package designs engineered to facilitate azimuthally omnidirectional acoustic signaling, as needed to implement the networked acoustic modem system. Next, results of preliminary field tests of acoustic modems are described in the context of a key question: at a separation of several kilometers, are error-free digital acoustic communications between nodes reliable at least several times daily? If so, the system should be considered to remain promising for purposes of the data assimilative numerical modeling requirements described above. The modem performance results indicate sensitivity to wind speed and raise the question of what conditions (wind speed, sound-speed profile, water depth, upslope/downslope directionality, tidal phasing) degrade modem communications. While comprehensive investigations of mechanisms responsible for performance degradation lie beyond the scope of the present work, some preliminary assessments are made.

Section 2 presents gateway and bottom frame engineering. Three field experiments implementing these devices and spanning a range of seasons and sound-speed profiles are described in section 3. Acoustic modem performance data are presented with analysis and interpretation in section 4 to quantify the

reliability of node-to-node communications at various internode ranges. Conclusions follow in section 5.

2. Bottom-mounted instrument frames and gateway buoy

a. Bottom-mounted instrument frames

Two primary design constraints must be satisfied by bottom-mounted instrument frames to facilitate a networked acoustic modem system in coastal areas that are subject to commercial fishing activities. They must permit azimuthally omnidirectional acoustic communications, and they must protect sensors against potential impacts of trawling gear. The frame presented here has been designed to achieve these objectives and to offer straightforward deployment and recovery operations.

Minimizing damage to oceanographic and fishing equipment is a concern in most coastal areas. The approach taken here is twofold. First, efforts are made to establish communication between scientists and fishers. Scientists learn the prevalent types of fishing equipment and techniques, and the most actively fished times of year, if seasonal. Fishers are informed that oceanographic equipment is planned for deployment and are encouraged to suggest potential sites for instruments near known boulder or wreck areas they avoid. A survey distributed to fishers in New York, Connecticut, and Rhode Island yielded valuable information to guide instrument design and placement. Regular announcements of deployment locations are made in the Local Notice to Mariners published by the Coast Guard. At the request of fishers, high-flyer radar reflectors are set as surface markers adjacent to all instruments to signal them to vessel traffic.

In addition to dialogue with the fishing community, efforts to limit damage to sensors and to fishing gear center on designing an instrument frame that deflects trawling gear on impact. This requires all components to be housed beneath the structural members of a low-profile pyramidal frame. Based on similar designs (e.g., Dessureault et al. 1991), including those that incorporate results of trawling tests, the face angle of the package is held to no more than about 30° above horizontal.

Azimuthally omnidirectional acoustic signaling from a transducer within the frame is critical for functioning of the acoustic modem network. This is necessary to send data along multiple bearings associated with various routes configurable from shore without requiring physical adjustment to the deployed instruments. It also eliminates the need for precise orientation of bottom frames during deployment, an important practical consideration. The combined needs for a low profile and azimuthally omnidirectional acoustics impose a stringent geometrical constraint on the frame design. The modem transducer must be at the frame apex and other components must be arranged at the base in order that they obstruct the transducer beam pattern minimally (Fig. 2a).

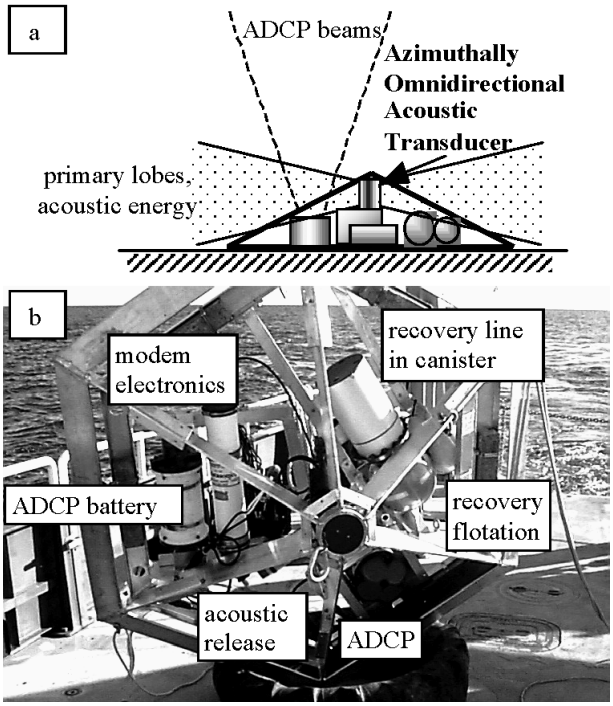

FIG. 2. (a) Schematic of bottom-mounted instrument frame design and function. The low-profile pyramidal shape helps deflect dragged trawling gear. To enable azimuthally omnidirectional acoustic communications, as required for flexible rerouting of data routes in the acoustic network, all components other than the acoustic modem transducer are arranged as far beneath it as possible. (b) Protoype UConn frame (''gazebo'') in upright position after recovery on the R/V *Connecticut.*

The frame houses three primary functional modules (Fig. 2b): the oceanographic sensor or sensors, the acoustic modem, and the recovery package. The frame is aluminum, ~70 cm high, and ~230 cm in diameter. To date, acoustic Doppler current profilers (ADCPs) have been incorporated; there is space for additional sensors. Selection of the ADCP model with a shortened pressure housing and an external battery pack permits their placement as far below the transducer beam pattern as possible. The model of acoustic modem used has its cabled transducer separate from its electronics pressure housing (''remote transducer'') for maximum hardware configuration flexibility. The azimuthally omnidirectional line-array transducer type is used for its potential to achieve greater horizontal range, due to its increased gain in the horizontal plane.

For deployment the frame is lowered using a heavy-duty acoustic release. Lack of a bottom surface on the frame minimizes kiting during lowering. Once on the bottom, the acoustic modem can communicate the frame pitch and roll angles, as measured by the ADCP, to a deck unit acoustic modem. An instrument deployed at an unacceptable angle can quickly be redeployed; tilt-

sensitive components are not gimballed because orientation angles can be confirmed remotely during deployment. Recovery is by pop-up float, launched by a lightweight acoustic release on the frame. On rising, the float pulls a lifting line from a packed canister, permitting diver-free retrieval of the package.

Panels covering the frame in an early design are now omitted based on the discovery of high sediment mobility at the shallow inshore portions of the site. In the initial design, sheets of ultra-high-molecular-weight plastic with acoustic impedance closely matched to that of seawater were secured across all faces of the frame to improve trawl resistance. At the end of an early deployment, a failed acoustic release required use of a remotely operated vehicle for recovery, which was carried out by the North Atlantic and Great Lakes office of the National Undersea Research Center at the University of Connecticut. Video images of the bottom frame after several weeks on site revealed sand and mud trapped inside the plastic panels had largely filled the pyramidal volume. Tidal currents are strong (reaching $\sim$50 cm s^{-1}) and most likely resuspend sedimentary materials, transporting them into the frame where they accumulated. Accordingly we omit panels from our design, sacrificing some trawl resistance but limiting sediment buildup. We note that a frame design incorporating properly ballasted solid syntactic foam (unlike that presented here) could provide a protective outer surface while also keeping sediments from filling it; such a design would need to ensure the foam does not interfere with the acoustic modem signaling.

In the context of the budget for this project, the expense of the bottom frame construction was only justified in order to protect a limited number of oceanographic sensors. Network nodes consisting of an acoustic modem deployed individually (e.g., repeaters) are in general less valuable (1/4 the cost or less), and do not store oceanographic data internally; hence, the decision was made to deploy them without trawl-resistant frames. These nodes were configured as short in-line moorings with the acoustic modem about 5 m off the seafloor and sub-surface flotation the shallowest element some 8 m off the seafloor (Fig. 3). As described below, a number of these nodes were lost, presumably due to fishing activity. Furthermore, during FRONT experiments at least three bottom frames were impacted by trawling gear. This was determined following their recovery based on obvious physical damage (deeply scraped aluminum; damaged recovery module components) and/or discontinuities in pitch/roll/heading time series recorded internally by the ADCP. A measure of success for the design and function of the bottom frames is that, in the course of more than 30 deployments and recoveries throughout the FRONT project, only one ADCP showed evidence of minor damage and none was lost. Given these results, the additional expense of trawl-resistant frames for every node, including repeaters, may well be justified in future deployments.

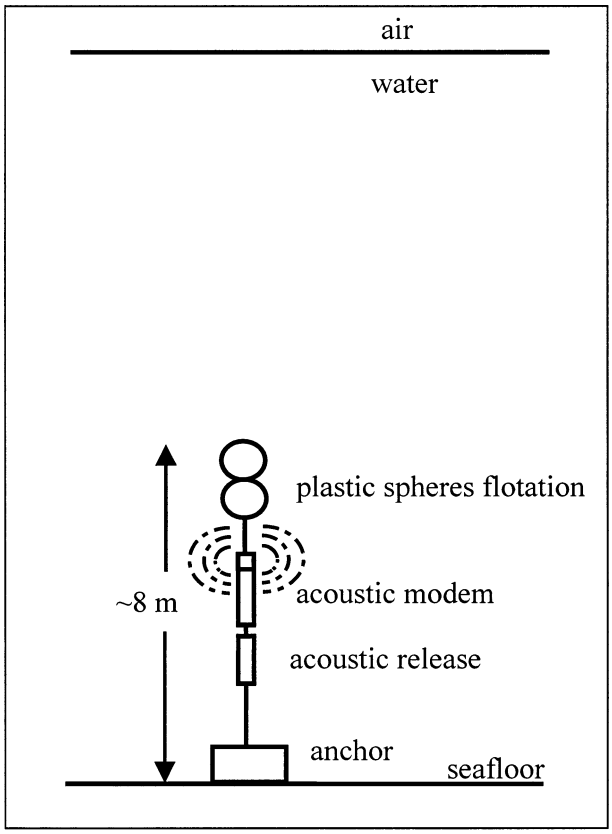

FIG. 3. Near-bottom in-line mooring configuration for network nodes consisting of individual acoustic modems only (referred to as repeaters and listeners).

b. Gateway buoy

The gateway node consists of a surface buoy with payload including a cellular telephone modem interfaced by serial cable to an acoustic modem, for which the transducer is submerged, and a battery power supply that is replenished by solar panels (Fig. 4a). Cellular modems are used because there is no need for a dedicated onshore station and the service is available at a flat monthly rate for unlimited data transmission. A 19.2-k cellular digital packet data (CDPD) link to the cellular modem, at its uniquely assigned IP address, is established via the Internet by a control center PC typically residing onshore (in this case, either in Groton, Connecticut, or San Diego, California). During cruises, the control center PC has resided on the vessel through use of one additional cellular modem.

The experiments presented here use a ''buoy of opportunity'' in the form of the Montauk Point U.S. Coast Guard (CG) navigation buoy (Fig. 4b). This has the advantage that the CG maintenance effort is leveraged, although the fixed position of the buoy hinders flexibility in placement and spatial configuration of the array. A second gateway, a buoy with an extended submerged portion for the acoustic modem transducer, is used in

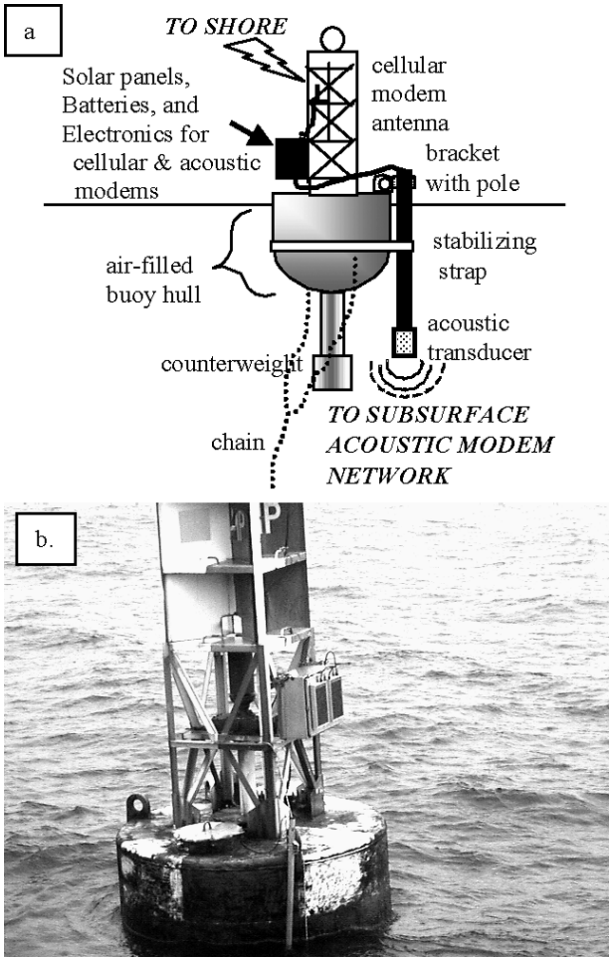

FIG. 4. (a) Schematic gateway node components as configured for a U.S. Coast Guard navigation buoy. Acoustic transducer is positioned 3 m deep at the end of a pole in order to minimize surface bubble effects and potential shadowing by the air-filled buoy hull. (b) Montauk Point buoy with the above design implemented.

later experiments (not discussed here) and enables more flexible array configuration.

For a gateway the most important feature is that the acoustic modem transducer is positioned as deep as possible. This minimizes acoustic absorption and scattering by bubbles associated with breaking surface waves, and limits the shadowing influence of the air-filled buoy hull. On the CG buoy the acoustic modem transducer is mounted at the end of a pole that is bracketed to a bail on the hull platform and stabilized with a strap around the buoy hull (Fig. 4b); the depth of the transducer is 3 m, the maximum possible as constrained by the need to avoid contact with the buoy chain bridle. To limit degradation of the gateway acoustic link, the nearest repeater or sensor modem is located within direct-path range, generally not more than about 100 m from the buoy.

Solar panels recharge batteries to supply power requirements of the cellular and acoustic modems, which are dominated by the cellular modem. The cellular connection is >99% error free when open, though unpredictable outages occur as an unavoidable aspect of the service. Though not implemented for the experiment described here, software to automate the reconnection process immediately following a cellular connection loss is incorporated in later experiments.

3. Field experiment configurations

Acoustic modem performance data are presented from three field deployments. They are denoted W99 (winter 1999, 5–13 December, FRONT-1), S00 (spring 2000, 20–28 April, ForeFRONT-2), and F00 (fall 2000, 26 October–10 November, ForeFRONT-3). The region for the deployments (Fig. 5a) is to the south and east of the Montauk Point Coast Guard buoy (marked MP in Fig. 1), which is used as the gateway node G1 in F00 as described in section 2b. For each deployment, the data sources are ADCPs in bottom frames (circles in Figs. 5b–d; node designation prefix A) of the type described in section 2a.

Repeater and listener nodes (diamonds in Figs. 5b–d; node designation prefixes L and R, respectively) are acoustic modems deployed individually as described above (Fig. 3). For W99 and S00 the acoustic modems deployed individually are termed ''listeners'' instead of ''repeaters'' because they logged data internally from packets they received but they did not have the ability to relay data packets; in F00, packet relaying was implemented so these nodes are referred to as repeaters. Placement of these modems near the seafloor is motivated by the fact that downward-refracting sound-speed profiles, which may reasonably be expected to prevail for much of the year, favor bottom-located nodes by increasing the horizontal range of a direct path. In addition, near-bottom deployment helps minimize risks of biofouling and tampering; although high flyers are set separately to serve as surface markers, mooring function requires no surface signature because acoustic releases are used for recovery.

Modems in W99 and S00 are Benthos (previously Datasonics) model 875 series. For F00 they are model 885 series with networking firmware developed for the navy's Seaweb 2000 (Rice et al. 2000) experiments. Modems operate at 9–14 kHz, with source-level 180 dB relative to 1 μPa at 1 m, net information data rate 300 bits per second (bps) and Hadamard and convolutional coding. Hadamard coding is implemented as block coding on multiple-frequency shift-keying (MFSK) modulation with six interleaved subsets of 20 frequencies each, 10 of which are active during transmission of a symbol; this provides frequency diversity to help overcome frequency-dependent fading and narrowband noise (Proakis 1991). Convolutional coding incorporates redundancy in the modulated symbols such that channel errors can be corrected at the receiver. Detailed information on the signal processing algorithms can be

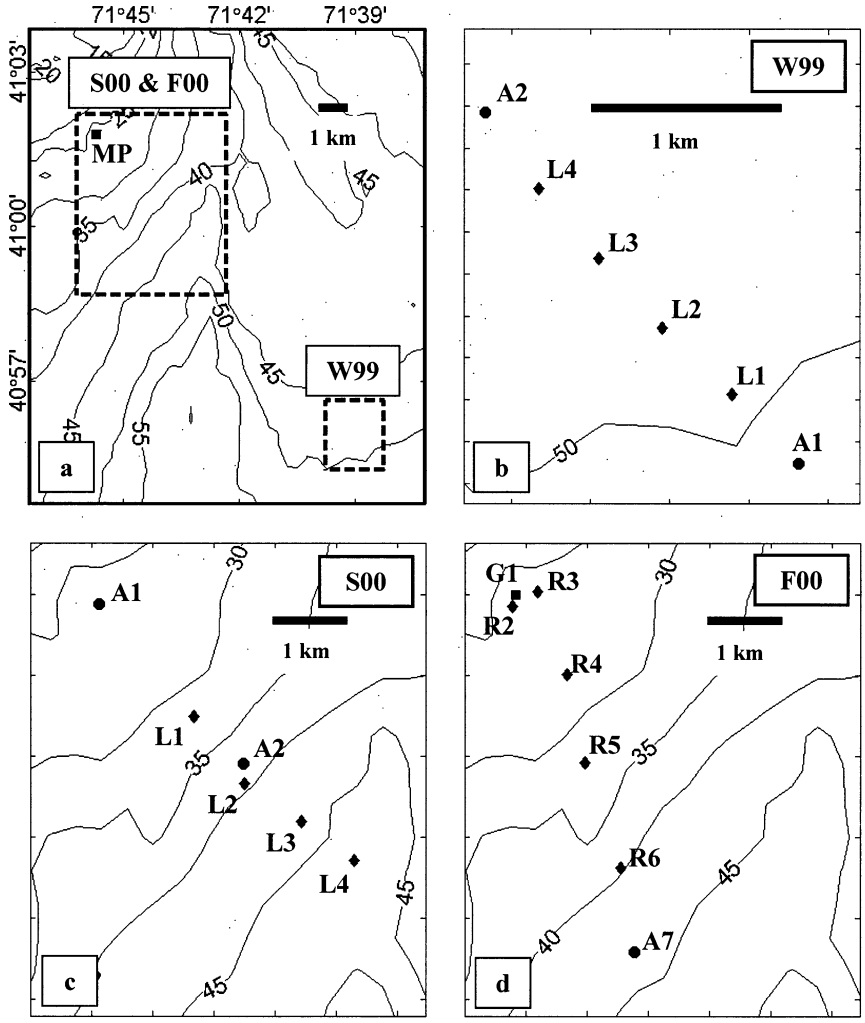

FIG. 5. Field experiment deployments. Scale marked in upper right of each frame. Isobaths labeled in meters. (a) Large-scale view of region; for reference, note Montauk Point USCG buoy appears here and in Fig. 1. (b) W99, (FRONT-1) experiment [lower-right inset from (a)]. (c) S00, (ForeFRONT-2) experiment [upper-left inset from (a)] (d) F00 (ForeFRONT-3) experiment [same inset as in (c)].

found in Scussel et al. (1997), Green et al. (1998a), and Rice et al. (1999). There are two types of transducers used (beam patterns available from the manufacturer): those in bottom frames, described here as azimuthally omnidirectional (model AT-409), and those on modems deployed individually (Fig. 3) and on gateways, described here as spherically omnidirectional (model AT-408).

The relatively low operating frequency is selected in order to maximize range, given the goals described in the introduction. Noncoherent MFSK is employed for channel tolerance and low-complexity signal processing. The choice of relatively low, fixed net information rate of 300 bps reflects a trade-off between the need for reliability over a variety of node-to-node distances and the need to transmit up to a few hundred bytes with reasonably short-duration (up to about 10 s) packets. A measure of communication channel capacity used to characterize continuous point-to-point links, such as those between microwave towers, is the throughput (given in, e.g., km kilobits kb s^{-1}). While this metric is not particularly appropriate for the light duty cycle of the FRONT network in which the channel is idle more often than it is used (see introduction), a representative value is 0.6 km kb s^{-1} determined as the product of the net information rate 300 bps and the nominal 2-km range between nodes. Interpretation of this traditional point-to-point measure of channel capacity can be misleading considering the multiple-access nature of the medium, the half-duplex nature of the link, the light duty cycle of the network, and the conservative bit rate selected.

Data sources are RDI Instruments Workshorse ADCPs with use of a flexible ADCP output format de-

veloped for this project and now incorporated in standard RDI firmware. It facilitates serial output of a subset of the temporal and vertical sampling, and a subset of the velocity components, to create appropriately sized packets for acoustic transmission; the standard format is simultaneously recorded internally for postrecovery analysis.

Winds used are from National Data Buoy Center buoy 44025 off Long Island, New York (40.25°N, 73.17°W). Winds from this buoy are of higher quality than those measured at other locations in the region. They are representative of the modem deployment site despite the fact that the buoy is located ~120 km away, due to the large wind coherence length scales along the New York, Rhode Island, and Massachusetts coastlines.

4. Acoustic modem performance

We report field results for modem performance at the FRONT site. Sensitivity of modem performance to the geometry of instrument placement is expected and is unlikely to remain static in time. Results below show performance degradation in association with elevated wind speeds. Among the numerous mechanisms that may be responsible are air–sea interface roughness; seabed roughness changes and/or noise associated with sediment movements driven by surface waves or tidal currents; increased numbers, changed size distributions, and/or depth penetration of bubbles; changing sound-speed profiles and/or surface ducting properties; varying ambient noise levels; or combinations of these. Auxiliary data to test hypotheses regarding these mechanisms were not collected. Improvements to performance will require future studies to address such processes; here, we present clear evidence of the connection between elevated wind speed and modem performance and comment briefly on potential mechanisms.

a. W99 (FRONT-1)

The winter 1999 experiment occurred in shelf waters between 46 and 51 m deep (Fig. 5a, lower-right inset) and involved two bottom-frame ADCPs, labeled A1 and A2, as sources 2.5 km apart and four listener modems, labeled L1–L4, at 0.5-km spacing linearly between the sources (Fig. 5b). Each source modem transmitted a 255-byte packet of ADCP data at 15-min intervals, offset by 7.5 min from the other. The listeners passively logged the data packets they received successfully to an internal buffer, which has been analyzed postrecovery.

Sound-speed profiles measured during the deployment cruise show monotonic increases with depth so the acoustic channel was upward refracting (Fig. 6a). The difference in sound speed from top to bottom was about 4 m s^{-1}, with the majority of the change occurring across the middepth interval from 30 to 35 m. The temperature profile (not shown) parallels that of sound speed, increasing with depth across the middepth transition layer, as a result of wintertime surface cooling; the associated destabilizing effect on the density profile is overcome by increasing salinity with depth (not shown) due to the freshening influence of the nearby estuaries on near-surface water.

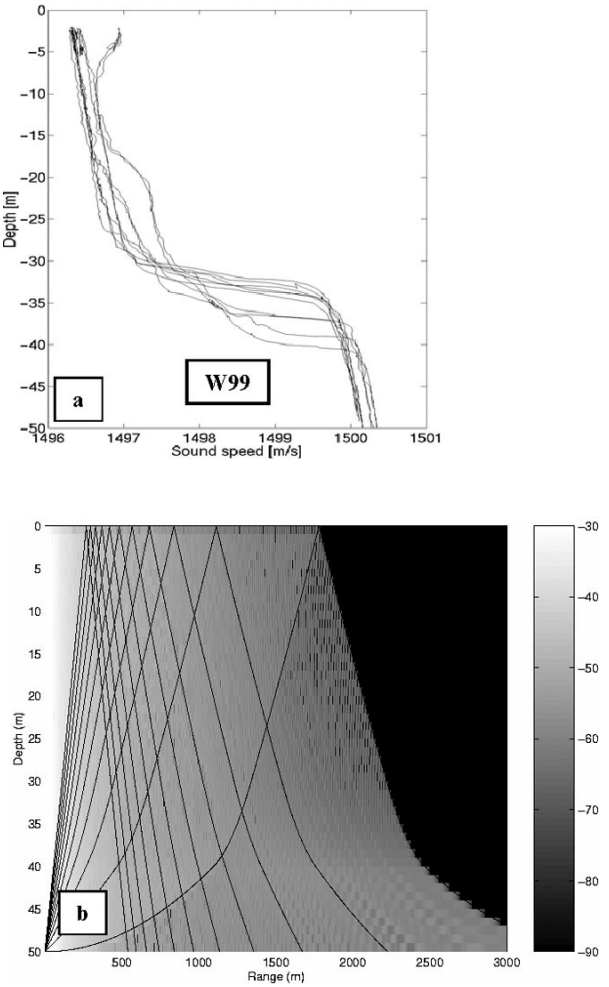

FIG. 6. (a) Upward-refracting sound-speed profile measured during W99. (b) Acoustic power (dB relative to source) as a function of depth and range for the source at bottom left of field of view, numerically modeled by rays, using average of sound-speed profiles in (a). All rays interact with the sea surface at short horizontal ranges. (Shadow zone forms at right because zero reflectivity of the seafloor has been assumed.)

As all modems were deeper than the abrupt increase of sound speed with depth, sound waves are expected to refract upward. Using an average sound-speed profile calculated from those in Fig. 6a, acoustic ray modeling calculations quantify the upward refraction (Fig. 6b). Rays from bottom sources are guided upward and incident on the sea surface at ranges of less than 2 km.

An 8-day time series showing packets transmitted by A1 that were received by each listener node and sensor node A2 (Fig. 7) suggests a strong dependence of modem performance on wind. When the wind speed ex-

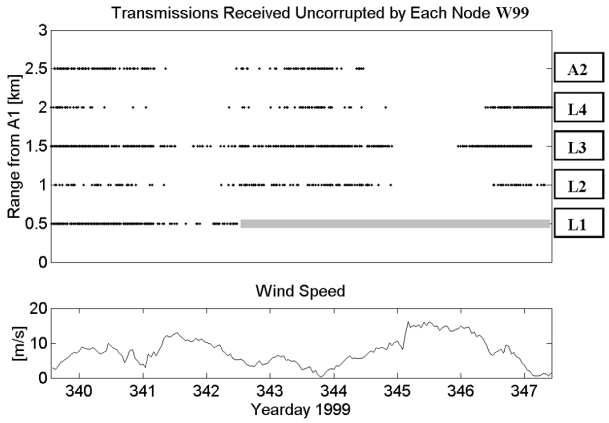

FIG. 7. W99 time series of modem performance. Symbols indicate receipt of uncorrupted packet from A1 as determined from data logged internally in each node. Horizontal gray bar indicates where L2 stopped collecting data early. Increased winds reduce successful communications.

ceeds about 10 m s^{-1} (primarily on yeardays 341 and 345) modems at ranges of 1 km or more receive far fewer packets uncorrupted. Even node L1, at a range of just 0.5 km from the source, is unable to receive well during the strong winds of yearday 341 (this node stopped logging data early when its buffer filled because it had not been cleared properly prior to deployment).

As expected for the variable channel properties described above, modem performance (Fig. 7) is not a simple monotonic degradation with increasing range. This is seen on inspection of the time series for L1–L4 and A2 relative to each other. Other than the shortened record at L1, the highest reliability is seen at L3, despite the fact that it is at larger range than L2. In addition, A2 outperforms L4, but only during the first 5 days of the record; during the last 2 days of the record, A2 receives no transmissions.

b. S00 (ForeFRONT-2)

The spring 2000 experiment occurred immediately to the south and east of the MP buoy (Fig. 5a, upper-left inset) in water depths of 26 to 47 m (Fig. 5c). Listeners were nominally 1 km apart. Similar to W99 the two sources alternated transmissions, in this case each 20 min, and the four listeners passively logged successful receipts internally for postrecovery analysis. Winds (not shown) during the 8-day experiment had similar strengths and variations as those during W99 (Fig. 7).

Sound-speed profiles measured during S00 showed a high degree of variability, including several with sharp middepth local maxima of up to 3 m s^{-1} faster than at other depths (Fig. 8a). On averaging across these variations, the pattern includes values decreasing with depth by up to 4 m s^{-1} in the shallowest 5–10 m, and increasing with depth by about 1–2 m s^{-1} from about 10 m deep to the bottom. The complicated variability is associated with competition between increased springtime surface warming due to solar insolation and estuarine input of relatively fresh, cold water in the upper water column; this is moderated by vigorous tidal currents that can cause local mixing, particularly in the shallower water depths as evidenced by the nearly uniform ($\sim$1471 m s^{-1}) profiles.

The average of the measured S00 sound-speed profiles includes downward refracting conditions in the shallowest part of the water column, which when used in ray modeling indicates that at least some rays will be ducted away from the surface (Fig. 8b). The deeper portions of the rays indicate upward curvature consistent with the slight increases in sound speed with depth there. Based on the modeled rays the expectation might be for the channel to be more reliable in S00 than in W99. However, the S00 time series performance (not shown) had similar dependence on wind speed to that of W99. Evidently, despite the fact that the ray paths in Fig. 8b are not incident on the sea surface, modem performance has been degraded by winds much as in W99.

The bulk performance of each node during the 8-day S00 experiment can be expressed as the percent of transmissions successfully received (Fig. 9). The results for both sources A1 and A2 reveal clearly the expected pattern of performance degradation with range. A minor deviation from the pattern is that L2 has outperformed A2 in receptions from A1 (Fig. 9, left panel) despite its larger range; this might be attributed to the different positions and types of the transducers (L2, a spherically omnidirectional unit at 5 m off the bottom; A2, an azimuthally omnidirectional unit in the bottom frame) except that the opposite performance was seen in W99, where A2 outperformed L4 (Fig. 8). As a result we consider this to be further evidence of geometry-dependent complexity of the channel. Finally, on comparing L1 and L3 receptions from A2 (Fig. 9, right panel), we note that the data do not reveal a strong asymmetry, for near-bottom sources and receivers, for transmissions to deep water from shallow as compared to transmissions from shallow water to deep.

In S00 more so than in W99 (or F00, discussed below) variability in the sound-speed profiles measured is high. This is likely attributable to tidal advection (e.g., Codiga and Rear) of sharp horizontal property gradients that can extend throughout the water column and are associated with estuarine outflow. The S00 experiment is therefore considered the most likely to reveal dependence of modem performance on tidal cycles. However, there is no tidal pattern in the time series of modem performance in any of the three experiments including S00 (not shown). Tidal processes are not a primary influence on modem performance at this site.

A composite summary of modem bulk percent success as a function of internode range independent of

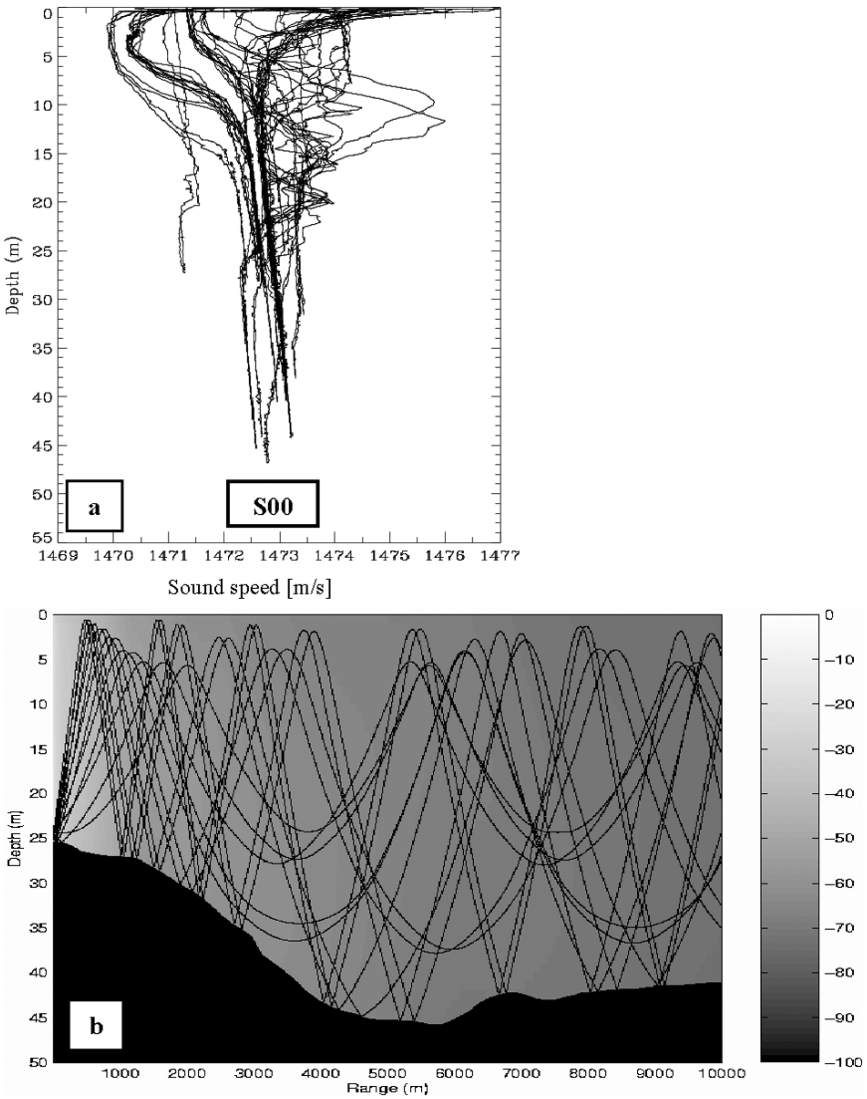

FIG. 8. (a) Sound-speed profiles measured during S00 at a range of locations spanning the modem positions. Variability is high and ducting appears possible in various depth regions for certain casts. In the shallowest 5 m, sound speed increases with proximity to the surface, suggesting the possibility of downward refraction there. (b) As in Fig. 6b, from the model incorporating bathymetry, with superposition of rays demonstrating that some are refracted away from surface.

node positions (Fig. 10) provides a quantitative measure of modem performance with which we can assess the viability of networked acoustic modems for the application discussed in the introduction. It should be borne in mind that the percent success values in Fig. 10 are based on an 8-day period and so are only representative of long-term performance to the extent that the environmental conditions during that 8-day period are representative. For example, the absolute level of the percent success values at all ranges would be lower had the 8-day period included higher than typical wind speeds. During the 8-day S00 deployment, the range at which modem receptions fell to a 50% success rate is between 2 and 3 km. This is marginally adequate in the context of the goals discussed above. Improvements on this S00 modem performance were achieved in F00 due to modem features, as described next.

c. F00 (ForeFRONT3)

The fall 2000 experiment occurred in the same region as S00 (Fig. 5a, upper-left inset), with instruments in water depths ranging from 26 to 44 m (Fig. 5d). There is one source node, A7, that transmitted a data packet each 40 min for 2 weeks. The ''repeater'' nodes (designated so, as opposed to ''listeners,'' because unlike

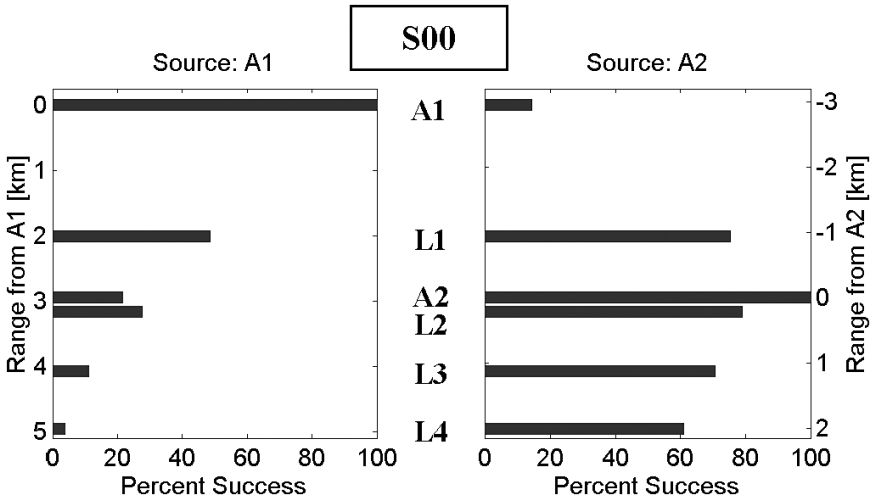

FIG. 9. Bulk success between various nodes for the 8-day duration of S00, with source nodes marked at 100% for reference. No strong asymmetry between up- and downslope communication performance is seen.

in W99 and S00 they act as relays, as described below) were placed nominally 1.2 km apart.

Sound-speed profiles measured during F00 (not shown) consistently exhibited weakly upward-refracting conditions in the shallowest 30–35 m, with sound speeds increasing downward by a total of about 1 m s^{-1}. Deeper than this, some casts showed no change relative to shallower water, while others revealed a strong decrease in sound speed by up to 7–8 m s^{-1} at the bottom. The latter situation appears to be associated with advection of a deep layer of cold water toward the site from offshore, upcoast, or downcoast. In summary, all modems except the deepest two (R6 and A7) are in a nearly constant sound speed, weakly upward-refracting water column; at least some of the time, the deepest two were in a deep layer that was strongly downward refracting.

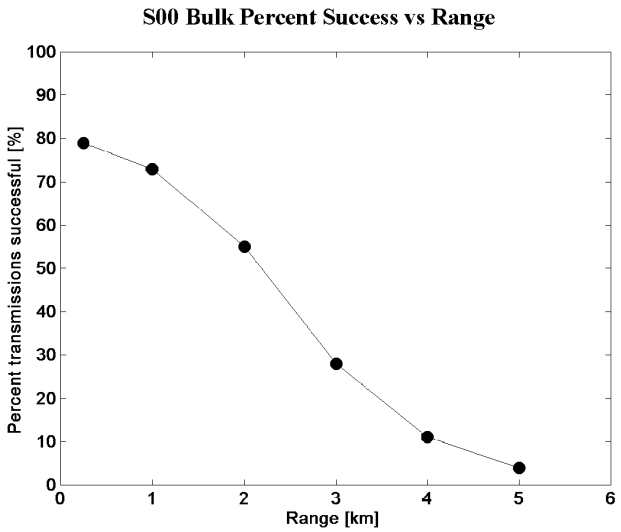

FIG. 10. Composite of values in Fig. 9, binned to 1-km ranges.

The deeper modems do not exhibit strongly different performance (Fig. 11, discussed below) that could be attributable to the intermittent downward-refracting deep layer.

1) DIFFERENCES FROM W99 AND S00 IN MODEM HARDWARE AND FIRMWARE

The F00 experiment incorporates several differences from W99 and S00 as a result of using different modem hardware and firmware. The hardware (Benthos model 880 series) is based on a more powerful microprocessor,

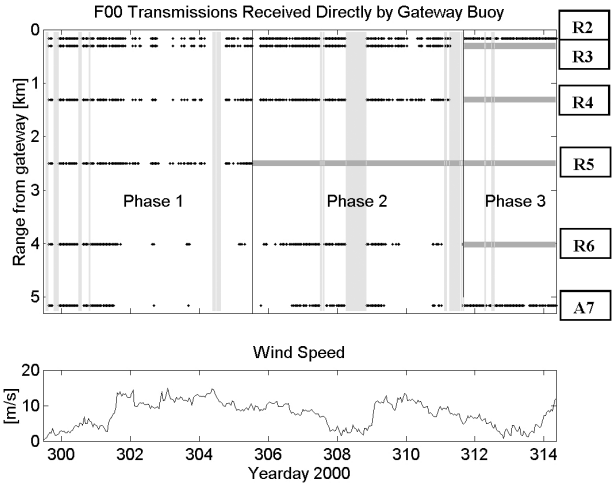

FIG. 11. Time series of reception of packets by gateway directly from each individual node during F00, as facilitated by receive-all mode. Gray horizontal bars denote when nodes are not part of the data packet routing: data routes for phases 1, 2, and 3 were A7–R6–R5–R4–R3–R2–G1, A7–R6–R4–R3–R2–G1, and A7–R2–G1, respectively. Gray vertical bars indicate time periods when the cellular modem link between the gateway and the shore was inoperable.

which enables the use of more sophisticated firmware. Several new firmware features developed during the Seaweb 2000 experiment in Buzzards Bay, Massachusetts (Rice et al. 2000), were implemented. First, the modems have networking functionality: a header for each message includes the final destination node, and each transmission is addressed to a specific node, so the route of a packet to its final destination can span several ''hops'' or node-pair transmissions. When a given node, for example a repeater, receives a message, it reads the final destination node from the header and uses its own internal lookup table to determine the node to which it will forward the message; the lookup table can be changed remotely through acoustic commands so that packet routing is reconfigurable from shore. Second, the wake-up processing algorithm is changed from 3-of-3 tone detection to 2-of-3, which proves to have substantially less vulnerability to narrowband fading and noise yet maintains a sufficiently low false alarm rate (Rice et al. 2001). Third, the communications protocol incorporates short utility packets that are a form of handshaking. A sending node initiates the exchange with a ''request to send'' (RTS) utility packed addressed specifically to the receiving node. The receiving node then replies with a ''clear to send'' (CTS) utility packet. The sending node then transmits the data only on successful receipt of a CTS from the receiving node. If no CTS is received in response to an RTS, up to five additional RTSs are sent in an attempt to establish the link. Finally, the MP buoy serves as a gateway and implements a ''receive all'' feature that effectively enables it to overhear transmissions between any two nodes. In this way, when a data packet is sent between each node pair along a route, the gateway receives the data ''directly'' if the acoustic channel permits; each data packet has multiple opportunities for reception by the gateway.

2) Bulk success rate

The bulk success rate of data packets reaching the gateway, a measure of the performance of the entire network of acoustic modems in delivering data from the source node to the shore, was 82% during the 2-week F00 period. Because the gateway is the final destination of each data packet and it is also in receive-all mode, it can receive a packet multiple times. Each packet originating from A7 is only counted once toward the bulk success rate. In order to distinguish from later relay transmissions, we refer to receipt of a packet by the gateway from any node, whether or not the source node, as ''direct'' when the sending node does not have the gateway as the first receiver in its route. For example, the initial routing of data packets is A7–R6–R5–R4–R3–R2–G1: A7 transmits to R6, then if R6 receives successfully it transmits to R5, and so on. The transmission from R6 to R5 has R5 as its first receiver, but can be received by the gateway ''directly'' because the gateway is in receive-all mode. In contrast, even if the acoustic channel was such that the gateway was not able to receive transmissions from any nodes other than R2, the packet may nonetheless arrive at the gateway; in this case it is received on the hop from R2 with G1 as its first receiver, and is therefore an ''indirect'' reception with respect to all other nodes. The 82% bulk success rate includes both direct (minimum ~65%) and indirect transmissions. Packets received by the gateway when the cellular connection was inoperable were not identifiable as direct or indirect due to the format of gateway buffer logging; they contribute only to the 82% value; hence, 65% is a minimum value for direct receipts [as discussed in section 4c(7) below].

3) Effect of winds

Time series of direct receipts by the gateway in receive-all mode, from each of the other nodes, together with the wind record, summarize the results of the F00 experiment (Fig. 11). The experiment had three phases, each of which incorporates different routing of data packets. In phase 1, data are routed as described above. In phase 2, data are routed as A7–R6–R4–R3–R2–G1 to bypass R5. In phase 3, data are routed A7–R2–G1. Horizontal gray bars in Fig. 10 indicate when a node was not part of the data route so receipt of data packets is not expected. Vertical gray bars in Fig. 10 indicate intervals of time when an outage made the cellular connection to the gateway from shore inoperable. During these intervals, the gateway stored data it received in an internal buffer, the contents of which were retrieved immediately on reestablishing the cellular connection.

Examination of phase 1 results in Fig. 11, with reference also to Fig. 7, underscores that degradation of modem range by elevated wind speed is severe and rapid. Low wind speeds during yeardays 300 and 301 permit a very high rate of successful transmission from all nodes directly to the gateway, including the source node itself at a range of more than 5 km. However, during high wind speeds, notably yeardays 302–304 and 310, the number of packets received directly by the gateway from all nodes is strongly diminished, including the two nodes that are less than 1 km from the gateway (R2 and R3). Increased winds degrade modem performance within at most several hours.

4) Demonstration of capability to reroute network from shore

The ability to remotely reroute network data pathways from shore, an important flexibility emphasized as an advantage of networked acoustic modems in the introduction, was demonstrated dramatically during the F00 experiment and proved critical to its successful completion. Phase 2 of the experiment was not planned in advance but rather began on inspection of the data in real time on yearday 305. It was noted that R5 had abruptly fallen silent and was not responding to any

RTS packets from R6, nor from R4. The conclusion was drawn that this node had either been damaged or removed through impact by a trawling vessel, or had failed due to a malfunction or battery depletion. In any case, its lack of operation was preventing the flow of data to shore.

From shore a sequence of commands was issued via the gateway node to reconfigure the routing to bypass R5. As established during the initial deployment, the routing for commands from shore to R2 was G1–R2, the routing for commands to R3 was G1–R2–R3, and so on. First, a command was sent to R4 to change the node to which it forwards messages with final destination R6 (and A7) to be R6 instead of R5. This changed the routing for commands to R6 from G1–R2–R3–R4–R5–R6 to G1–R2–R3–R4–R6 (and similarly for A7). It was possible then to send a command to R6 to change the node to which it forwards messages with final destination G1 to be R4 instead of R5. This changed the routing for messages to G1 from A7 to be A7–R6–R4–R3–R2–G1, as it remained for the duration of phase 2. A similar sequence of commands issued from shore was used to change the routing to initiate phase 3.

Loss of oceanographic equipment to trawling activities is in no way a desirable outcome. However, given the need for measurements to be made in heavily fished coastal areas, it is unlikely such events can be avoided altogether in the future. A system is needed that can react flexibly to such events. Here, responsiveness of the networked acoustic modem system to loss or failure of an individual node has been demonstrated.

5) VALUE OF RECEIVE-ALL GATEWAY MODE

An important difference between the time series of Fig. 11 and Fig. 7 is that the former was collected in real time, not postrecovery, as facilitated by the receive-all gateway mode. The benefit of this was made particularly clear when, during the recovery cruise, repeater nodes R3, R4, and R5 did not return to the surface on sending the command to fire their acoustic releases. Use of a remotely operated vehicle (S. Gallager, Woods Hole Oceanographic Institution, 2001, personal communication) on a subsequent cruise confirmed the modems were absent, noting also evidence of trawling impacts on the nearby bottom substrate. This eliminated the possibility that the repeaters were still present with failed acoustic releases. Repeater modems had logged data to internal buffers for use in postrecovery analysis, but these data were not recovered. Therefore it is the gateway receive-all capability that enabled the entire analysis of the network (Fig. 11). In a network with multiple gateways, each can be operated in receive-all mode. However, nongateway nodes in receive-all mode are problematic unless they only log their receive-all receptions internally for postrecovery analysis; if multiple nongateway nodes in receive-all mode forwarded received packets, a single transmission could then cause a cascade of multiple redundant packets and undesired network traffic and associated power drain.

TABLE 1. Number of transmissions resulting in repeated RTS and/or CTS packets.

Handshake sequence	No. of occurrences
R–R–C–D	20
R–C–R–C–D	11
R–C–R–C–R–C–D	2
R–R–R–C–D	1
R–R–C–R–C–D	1
Total	35

6) HANDSHAKING PROTOCOL

The lower bound for the number of node-pair transmissions involving multiple RTS, multiple CTS, or multiple RTS and CTS handshake utility packets was 3%. This is based on analysis of the gateway receive-all record. It is a lower bound because most receive-all data are recorded when winds are low, so there are few multiple RTS/CTS retries; when winds are high and RTS/CTS retries are expected to be both more common and more important for successful data throughput, the gateway is unlikely to log them. A handshake that is successful on first attempts consists only of an RTS packet from the sending node, a CTS packet from the receiving node, and a data packet from the sending node; this sequence can be represented symbolically as R–C–D. The total number of instances in which the handshake consisted of a sequence other than R–C–D and ended with a successful data transmission was 35 (3% of total transmissions); of these the most common type was R–R–C–D, which occurred 20 times (Table 1).

7) RELIABILITY AT LARGER RANGES

Direct gateway receptions from each of the nodes (Fig. 11) can be summarized in bulk success rates as a function of range (Fig. 12). All nodes, at ranges between 0.2 km and more than 5 km, had bulk success rates for direct reception at the gateway of between 42% and 65% during the 2-week interval. The severity of range-limiting winds is underscored by this result, since it demonstrates that even the nodes at very short range (R2 and R3) are unable to reach the gateway during high winds. While motion of the transducer on the buoy during high winds may contribute, it is unlikely to be wholly responsible since similar sensitivity to wind was seen in W99 between bottom-located modems (Fig. 7). Figure 12 invites an overly simplistic interpretation of acoustic modem performance as either ''on'' or ''off'' between all nodes within about 5 km, depending on whether the wind speed is low or high.

Figure 12 also reveals that, while there is a clear pattern of increasing success rate with reduced range as expected, the overall span of values from 42% to 65%

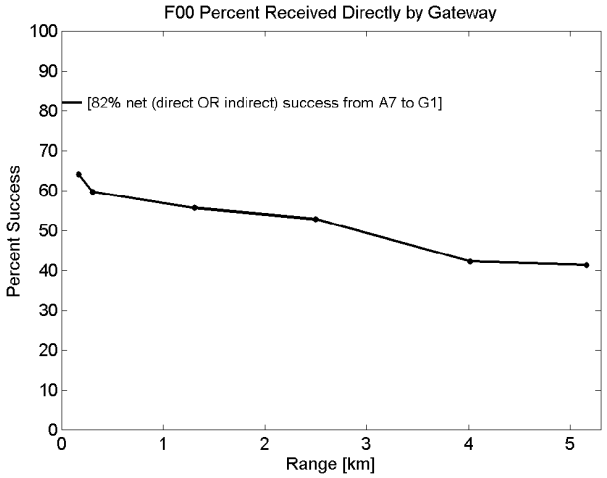

FIG. 12. Composite of values in Fig. 10. Net (direct or indirect) success in delivery of packets from A7 to G1 (82%) is shown; this exceeds that of individual nodes in part because of periods when G1 received packets from nodes at larger ranges and not at smaller ranges, e.g., in the early part of yearday 310 (see Fig. 11).

is much smaller than seen in earlier experiments, for example, S00 (Fig. 10). This demonstrates a substantial improvement for the modems at greater ranges, on consideration of the similar range of wind speeds seen during S00 and F00. Specifically, at a range of 5 km the percent success has increased from less than 5% in S00 (Fig. 10) to 42% in F00 (Fig. 12). While the F00 experiment provides no time series data to confirm that this is the case, it appears that the falloff of the percent success to, say, 25% or less may in fact be at a much larger range of up to 8 or 10 km. The improvement at large range is attributed primarily to improved signal detection algorithms in the 880 series modems [section 4c(1)]; handshaking retries took effect as little as 3% of the time (previous subsection) and so appear to be of secondary importance.

Reliability of communications between two nodes 5 km apart, both deployed at the bottom, is shown to be high through a period of mixed wind speeds (phase 3; Fig. 11). During this phase source node A7 routed its data to R2 directly, then R2 sent to G1. If the A7–R2 link was not successful, the R2–G1 link would not be heard. So the data packets received by G1 from R2 during this phase are indications that the A7–R2 hop was successful. The reliability of this hop during phase 3 demonstrates that the success rates depicted in Fig. 12 for large ranges are not dependent on the receiving node, G1, being near the surface, but rather are representative of bottom-to-bottom communications.

Finally, a comment on the difference between the bulk success rate of 82% [section 4c(2)] and the highest value of ~65% in Fig. 12. The former includes both direct and indirect data packets whereas the latter is for packets received only from R2 (indirects). An example of the distinction is seen early during yearday 310 (Fig. 11), when there were receptions directly from R4, but not from R2 or R3; these contributed to the 82% value only. Additionally, when the cellular connection was inoperable, both direct and indirect packets were received by the gateway, but because of the gateway log format, these were not identifiable by direct source and count only in the 82% value.

5. Conclusions

Networked acoustic modems present a means for real-time delivery of water-column measurements from multiple sparsely distributed instruments in the coastal ocean (Fig. 1). Developing a system for such a capability is made difficult not only by the unforgiving nature of strong winds, tidal currents, and sediment movement that typify coastal areas but also by the prevalence of heavy commercial fishing and shipping traffic, which make bottom cables and surface moorings problematic. In concept, a wireless undersea network of acoustic modems has many advantages in addressing this challenge. It includes a minimal number of gateway nodes, which are the only elements exposed to the difficult sea surface environment; it incorporates flexibility in network configuration through use of ''repeater'' nodes whose sole purpose is to relay data; and it has the ability to modify data pathways from shore, for example, to recover from damage or loss of an individual node without disrupting the entire network. We have presented results of initial development and testing efforts to determine the feasibility and initial field performance of acoustic modems in this networked application.

A trawl-resistant bottom-frame design (Fig. 2) has been developed that enables azimuthally omnidirectional acoustic signaling as required by the network. The frame makes deployment, and diver-free recovery by popup flotation activated by acoustic release, straightforward. Gateway buoys, the choke point for data flow between the underwater network and shore, require a cellular modem interfaced to an acoustic modem, with batteries replenished by solar panels. This has been implemented on a U.S. Coast Guard navigation buoy (Fig. 3), where the acoustic modem transducer is mounted 3 m deep at the end of a pole as is necessary to best remove it from the detrimental influence on its acoustic performance of surface bubbles and the air-filled buoy hull.

In the context of the commonly faced need to provide measurements to a data assimilative numerical model of coastal processes, a typical requirement from a real-time delivery system is the collection of data several times daily from several instruments deployed across at least a 10–20-km area. Networked acoustic modems will be cost effective in this application only if reliable acoustic communications can be established at horizontal ranges of at least several kilometers. Given the known hostility of the acoustic channel in shallow water, the feasibility of networked acoustic modems therefore

depends on whether they can achieve reliability across such ranges in coastal areas.

To help address this question we have presented results of acoustic modem performance during field experiments in a variety of different conditions (Fig. 5). The experiments span water depths from 26 to 51 m; the winter, spring, and fall seasons; sound-speed profiles with both upward- (Fig. 6) and downward-refracting (Fig. 8) characteristics; and a range of wind speeds up to 18 m s^{-1} (Figs. 7 and 11). Patterns in modem performance appear to be robust across this range of conditions.

In an experiment implementing improved modem features [section 4c(1)], we find a 42% success rate at 5-km range for data packets a few hundred bytes in size transmitted each 40 min during a 14-day fall experiment for which there was a predominately upward-refracting sound-speed profile and a range of weak and strong wind speeds (Fig. 12). Reliability of 42% at a range of 5 km, under the adverse conditions of an upward-refracting channel and reasonably strong winds, is sufficiently high to imply that a networked acoustic modem system remains a viable solution to address the data assimilative modeling needs stated above. The main drawback is that successful communications occur primarily at low wind speed; when winds are strong for more than a day, communications are disrupted for that duration (Fig. 11) so data cannot be delivered several times daily. It appears that the most promising functions that could be developed to improve the network in terms of overcoming this limitation are 1) the ability to operate in store-and-forward (e.g., Talavage et al. 1994) or ''meteor burst'' mode, so that when the channel clears, the backlog of unsuccessfully transmitted data can be sent, and 2) dynamic control of signaling parameters based on probe signals, or ''adaptive modulation'' (Rice et al. 1999).

On examination of experimental time series records (Figs. 7 and 11) high wind speeds are clearly associated with diminished performance. Wind-driven degradation in performance takes effect within hours of increased wind speed levels and occurs under all experimental conditions encountered. The extent to which strong winds degrade modem performance is severe, as emphasized by the reduced reliability they cause at all instrument separation ranges including those of less than 1 km. A number of mechanisms (listed at the start of section 4) may be responsible; to assess their relative importance would require auxiliary measurements (such as wave height and ambient noise level) that were not recorded. We note that the present results suggest that the dependence of modem performance on sound-speed profile, water depth, upslope/downslope directionality, and tidal phase appears to be secondary to the wind. A range of upward- and downward-refracting sound-speed profiles, and temporal fluctuations in them brought on by advection of different water masses to the site, has been spanned by the experiments. Even when partial ducting away from the surface occurs (Fig. 8), there is sensitivity to wind speed. There is little evidence for sensitivity of performance on water depth, or on whether the direction of transmissions is from shallow to deep water or from deep water to shallow water (Fig. 9). Although the site of these experiments has strong tidal currents as a result of their location at the mouth of a large estuary, little dependence of modem performance on tidal phase is seen.

Modem performance, in particular at larger ranges, has improved substantially with upgraded digital signal processing hardware and firmware algorithms. This is seen clearly in the comparison of performance between two different generations of modems in the S00 (Fig. 10) and F00 (Fig. 12) experiments. Certain networking functions were demonstrated in the most recent of the experiments reported here (F00). These include a ''request to send''/''clear to send'' (RTS/CTS) handshaking protocol, a ''receive all'' mode for the gateway to enable it to overhear all network communications, and reconfiguration of data routing by issuance of commands from a shore-based control center.

The RTS/CTS handshaking protocol provides an improvement to the modem performance by enabling more than one attempt to establish the link between each node pair. During F00, RTS/CTS was useful in at least 3% of the transmissions, a lower bound. The real value of handshaking is realized when the channel is adverse, such as when winds are strong; the data used to determine the 3% lower bound were collected by the gateway and are primarily from low-wind periods so they do not fully reflect the potential utility of the handshaking. Though it was not implemented here, a more complete handshake has been developed; in addition to the RTS/CTS exchanges it allows the receiving node to send an ''automatic repeat request'' (ARQ) utility packet, should it receive a data packet that has uncorrectable bit errors. On receipt of an ARQ, the sending node resends the data, thereby increased the chance for success. The number of ARQ retries allowed is a selectable parameter. Field tests of the performance of the RTS/CTS/ARQ handshake have been performed and will be presented in a future publication.

The receive-all feature for the gateway modem demonstrates two main utilities. First, it is a means of gathering information on performance of many nodes in the network in real time. If nodes should be lost, as occurred in F00, their internal buffer contents are not recovered so that the gateway receive-all record facilitates the only possible analysis of their performance. Second, the receive-all ability of the gateway to overhear transmissions between all node pairs increases the net success of delivery from a network because there are multiple redundant opportunities for gateway reception of a packet. In F00, for example, while R2 had a 65% success rate to G1, the network overall achieved 82% success, with the difference contributed to by packets that were received by G1 in receive-all mode from more distant

nodes such as R4, despite the failure of the transmission from R2 to G1.

The ability to reroute data pathways in real time by sending commands from shore to the undersea network has been demonstrated. Loss of a repeater node to trawling activity occurred midway through the F00 experiment, disrupting the data flow. A sequence of commands was sent from shore to the remaining network nodes via the gateway buoy, to reroute data pathways around the missing node. This process illustrated that networked acoustic modems facilitate a rapid response to such an incident from shore, an important capability given that no system can be completely invulnerable to failure or loss of individual nodes.

A final observation is that the real-time communications facilitated by deploying acoustic modems with moored instruments has practical benefits independent of their use as part of a network for real-time data delivery. There is a much lower likelihood of arriving on site to recover an instrument several months after its deployment, only to find that it was not properly recording data; feedback on the success or failure of instrument operation is immediate and enables responses to be made accordingly.

Acknowledgments. The experiments succeeded due to efforts of many who participated in and supported instrument design and field activities: Captain T. Cabaniss, D. Nelson, and the R/V *Connecticut* crew; D. Arbige, J. Bean, P. Bogden, L. Burch, D. Cohen, S. Colin, R. DeGoursey, R. Dziomba, J. Godfrey, G. Grenier, A. Houk, and D. Rogers of UConn Marine Sciences; I Babb, M. Slaney, and N. Worobey of NURC-NAGL; B. Creber, C. Fletcher, and V. MacDonald of SSC-SD; M. Porter of SAIC; T. de Groot, J. Hardiman, D. Porta, and K. Scussel of Benthos; and CWOs D. Tribou and T. Dillman of the USCG. Dale Green helped better relate this work to existing literature. This project is sponsored by the Office of Naval Research through the National Ocean Partnership Program (Award N00014-99-1-1020), an innovative collaboration of 12 federal agencies whose mission is to promote cooperative activities among the government, academia, industry, and other organizations for the advancement of ocean science, technology, and education. Cost sharing for involvement of U.S. Navy personnel was provided by ONR 321SS (Don Davison) and by the SPAWAR Systems Center San Diego Seaweb Initiative.

REFERENCES

Catipovic, J., 1990: Performance limitations in underwater acoustic telemetry. *IEEE J. Oceanic Eng.,* **15,** 205–216.

——, D. Brady, and S. Etchemendy, 1993: Development of underwater acoustic modems and networks. *Oceanography,* **6,** 112–119.

Codiga, D. L. and L. V. Rear, 2003: Observed tidal currents outside Block Island Sound: Offshore decay and effects of estuarine outflow. *J. Geophys. Res.*, in press.

Curtin, T. B., J. G. Bellingham, J. Catopovic, and D. Webb, 1993: Autonomous oceanographic sampling networks. *Oceanography,* **6,** 86–94.

Dessureault, J., D. J. Belliveau, and S. W. Young, 1991: Design and testing of a trawl-resistant package for an acoustic Doppler current profiler. *J. Oceanic Eng.,* **OE-16,** 397–401.

Frye, D., K. von der Heydt, M. Johnson, A. Maffei, S. Lerner, and B. Butman, 1999: New technologies for coastal observatories. *Sea Technol.,* **40** (10), 29–35.

Green, M. D., J. A. Rice, and S. Merriam, 1998a: Implementing an undersea wireless network using COTS acoustic modems. *Proc. MTS Ocean Community Conf.,* Vol. 2, Baltimore, MD, MTS, 1027–1031.

——, ——, and ——, 1998b: Underwater acoustic modem configured for use in a local area network. *Proc. IEEE Oceans '98,* Vol. 2, Nice, France, IEEE, 634–638.

Kilfoyle, D. B., and A. B. Baggeroer, 2000: The state of the art in underwater acoustic telemetry. *IEEE J. Oceanic Eng.,* **25,** 4–27.

Proakis, J. G., 1991: Coded modulation for digital communications over Rayleigh fading channels. *IEEE J. Oceanic Eng.,* **16,** 66–73.

Rice, J. A., 1997: Acoustic signal dispersion and distortion by shallow undersea transmission channels. *High Frequency Acoustics in Shallow Water,* N. G. Pace et al., Eds., Conf. Proc. Series P-45, NATO SACLANT, 435–442.

——, V. K. MacDonald, M. D. Green, and D. Porta, 1999: Adaptive modulation for undersea acoustic telemetry. *Sea Technol.,* **40** (5), 29–36.

——, and Coauthors, 2000: Evolution of Seaweb underwater acoustic networking. *Proc. MTS/IEEE Oceans 2000,* Vol. 3, Providence, RI, MTS/IEEE, 2007–2017.

——, R. K. Creber, C. L. Fletcher, P. A. Baxley, K. E. Rogers, and D. C. Davison, 2001: Seaweb underwater acoustic nets. Biennial Review, Space and Naval Warfare Systems Center San Diego Tech. Doc. TD 3117, 11 pp.

Scussel, K. F., J. A. Rice, and S. Merriam, 1997: A new MFSK acoustic modem for operation in adverse underwater channels. *Proc. IEEE Oceans '97,* Vol. 1, Halifax, NS, Canada, IEEE, 247–254.

Stojanovic, M., 1996: Recent advances in high-speed underwater acoustic communication. *IEEE J. Oceanic Eng.,* **21,** 125–136.

Talavage, J. L., T. E. Thiel, and D. Brady, 1994: An efficient store-and-forward protocol for a shallow-water acoustic local area network. *Proc. IEEE Oceans '94,* Vol. 1, Brest, France, IEEE, 883–888.

Ullman, D., and P. Cornillon, 1999: Satellite-derived sea surface temperature fronts on the continental shelf off the northeast U.S. coast. *J. Geophys. Res.,* **104,** 23 459–23 478.